SUPPLEMENTARY APPENDIX

PRECLINICAL DATA 2
Endothelialization 2
PARTICIPANT 3
Ethics and regulatory approval 3
Recruitment 3
Patient reported outcomes 3
IMAGING-GUIDED DEVICE DELIVERY 4
Pre-operative MRI acquisition (MRI venography and functional MRI) 4
Co-registration of deployment target markers for implantation 4
Endovascular device deployment 5
DECODER 6
Parameter optimisation 6
General design 7
Preprocessing layer 7
Classification layer 8
Click-logic layer 8
Multiclass classification 8
TASKS AND DIGITAL DEVICE CONTROL 9
Performance testing 10
Instrumental Activities of Daily Living (IADL) tasks 10
SUPPLEMENTARY TABLES AND FIGURES 12
Table 1. Inclusion and exclusion criteria 12
Table 2. Trial average system control performance 14
Figure S1. Implantable components 1
Figure S2. Endothelialisation of Stentrode implanted in chronic animal trial 2
Figure S3. Custom decoder 3
Figure S4. Motor mapping of movement-attempts 4
Figure S5. Classification of various movement-attempt types 5
SUPPLEMENTARY VIDEOS 6
Video S1. Neurointerventional procedure and device implant vignette 6
Video S2. Motor neuroprosthesis performance and utilisation vignettes 6
REFERENCES 7

Oxley TJ, *et al. J NeuroIntervent Surg* 2020;0:1–7. doi: 10.1136/neurintsurg-2020-016862

PRECLINICAL DATA

Endothelialization

An animal study was performed to demonstrate rates of endothelialization using an identical test article to that implanted in the human participant. Experiments were performed in accordance with FDA Regulations of Good Laboratory Practices for Nonclinical Laboratory Studies CFR Title 21 Part 58 and applicable NIH and NCI Standard Operating Procedures. Sheep (Merino ewes), were implanted with a Stentrode within a clinically-relevant sized vessel (6 mm jugular vein). The Stentrode was delivered using the coaxial catheter system designed for human use, and animals were terminated at day 3 (n=2) and day 45 (n=4), perfused, stained with Haematoxylin and Eosin and embedded in plastic or paraffin (APS, MN). 3-day subjects presented with completely denuded endothelium and thin segmental fibrin deposition. Although endothelial tissue loss presented, there was no exhibited injury to the vascular walls, deemed typical of an acute time point by the contracted agency. 45-day subjects demonstrated maturation of neointimal tissue that was expected of an extended time point. Microscopic fibrin deposition was observed on the intima and struts of the recording head, with 95% of device covered by 45 days (**Fig. S1**)**.**

PARTICIPANT

Ethics and regulatory approval

This was a first-in-human, single arm, open-label, prospective study approved by the Human Research Ethics Committee of St Vincent's Hospital, Victoria, Australia, in November 2018. Subsequent Research Governance Office approval was granted by The Royal Melbourne Hospital in January 2019. The Research Governance Office approval for the clinical recruiting site, Calvary Health Care Bethlehem, was granted in December 2018. Approval was granted under the Clinical Trial Notification (CTN) scheme of the Therapeutic Goods Administration (TGA) Australia (CTN Repository CT-2018-CTN-02369-1 v1.0) on 29th November 2018.

Recruitment

As per the inclusion criteria, participants with a motor score of >4/5 must report a subjective decline of upper limb extremity in the preceding four months resulting in functional impairment. The participants underwent screening to confirm eligibility and consented to the study. Inclusion criteria were satisfactorily met, including assessment of an fMRI demonstrating activation of primary motor cortex immediately adjacent to the superior sagittal sinus as well as an MR head and neck venography that demonstrated bilateral patent transverse sinuses and jugular veins by an interventional neuroradiologist (PM) and vascular neurologist (BC). Participants were assessed by a neurologist specialising in frontotemporal dementia (SL) to exclude dementia and assess capacity for informed consent. A respiratory assessment including pulmonary function tests and sleep study was performed. If follow up appointments satisfied anesthesia screening criteria the participants would progress to a final confirmation of suitability for general anesthetic and suitability for the procedure 2 weeks before implant. All other inclusion criteria were confirmed on day -1, with no exclusion criteria being met and the participant underwent the implantation via angiography. The participants were commenced on aspirin 300 mg daily and 75 mg of clopidogrel 14 days prior to the procedure. For participant 1, a point-of-care antiplatelet resistance test was performed seven days prior (VerifyNow, Accumetrics, CA), which revealed 11% resistance to clopidogrel. The decision was made by the treating interventional neuroradiologist (PM) to increase the dose to 150 mg daily. Repeat testing immediately prior to the procedure revealed adequate platelet inhibition of 30%.

Patient reported outcomes

Participant 1

At baseline, quality of life score (EQ-5D-5L) of 73 out of 100, reduced to 72/100 at day-7 post implant, and 70/100 at day-14 post-implant. This was maintained to month-4 follow-up and reduced at month-5 and month-6 follow-up at 65, further

reducing to 50/100 at month-12 follow-up. Hospital Anxiety and Depression Scale (HADS) score at baseline was D=3 and A=5. Over the duration of the trial a normal HADS score was maintained, although elevated compared to baseline (A=6/D=7) at month-12. Visual Analogue Scale (VAS) score, at baseline 0 out of 10, elevated post procedure to 1/10 from day-7 to day-21 post implant, returning to baseline from day-28 to month-5. VAS score increased at month-6 to 2/10 and 3/10 at month-12, with the patient reporting muscle pain secondary to progression of motor neuron disease.

Participant 2
The baseline quality of life score (EQ-5D-5L) was 45/100, increasing to 70/100 post-implant at day-14 follow up, reducing at day-28 to 65/100, increasing for month-2 and month-3 to 70/100 and reducing to 65 at month-4 follow up visit. Visual analogue numeric pain distress scale (VAS) at baseline scored 0/10. During follow-up the VAS was elevated at day-28 to 2/10 and returned to baseline for month-2 and month-4. HADS score measured at baseline of D=2 and A=5 and maintained normal levels throughout to month-4 follow up (A=3 D=2).

IMAGING-GUIDED DEVICE DELIVERY

Pre-operative MRI acquisition (MRI venography and functional MRI)

A pre-operative MRI investigation of the cortical and vascular structures, and cortical motor function was performed inside a Siemens MAGNETOM Prisma 3T scanner. The participant's vital signs were monitored, and communication was achieved through a two-way intercom while he was inside the scanner. The structural volumes were acquired using a contrast-enhanced (C+MPRAGE) and non-contrast enhanced magnetization prepared rapid gradient echo (MPRAGE) sequence, and contrast-enhanced Time-resolved angiography With Interleaved Stochastic Trajectories (TWIST) sequence. The acquired volumes were utilized to inform decisions regarding participation eligibility and implantation planning. Two sets of functional volumes were acquired using a gradient-echo echo-planar imaging (GE-EPI) sequence while the participant performed a lower-limb motor task. The participant was presented with instructions on the screen to either "rest" or "attempt". The task in the first and second set was to tap their right foot (repeated ankle plantar flexion and relaxation) and left foot, respectively, at a rate of ~1 Hz. Both rest and attempt blocks lasted for 15 s each. There were eight attempt and nine rest blocks as each experiment began and finished with a rest trial. The participant practiced the task outside of the scanner and were given verbal instructions prior to the scan via the intercom.

Co-registration of deployment target markers for implantation

Regions of significant Blood-Oxygenation-Level-Dependent (BOLD) signal fluctuation during the left and right lower limb movements were identified by fitting

a General Linear Model (GLM) to each dataset. *Z*-score maps were generated by contrasting the attempt and rest blocks for each functional set. The resulting BOLD activation maps for left and right foot tapping were co-registered to the C+MPRAGE space. The dorsomedial Primary Motor Cortex (M1) was identified in the C+MPRAGE volume based on the structural information and guided by the functional information by a neuroradiologist (PM). Three guide markers for device deployment were identified in the C+MPRAGE space. The portion of the superior sagittal sinus (SSS) immediately superior to the posterior margin of the dorsomedial M1 was marked (i.e., M1 marker). The anterior and posterior markers were placed 18 mm anterior and 22 mm posterior to the M1 marker, respectively (A and P marker; the total length of the recording head is 40mm). These markers encompassed portion of the Supplementary Motor Cortex (SMA), the M1 and the Primary Somatosensory cortex (S1), denoting the ideal deployment region of the stent electrode array for recording motor-related signals[1,2]. The C+MPRAGE volume with the three device deployment targets was co-registered to the pre-contrast 3D-Digital Subtraction Angiography (3D-DSA) volume acquired intraoperatively. Siemens' automatic co-registration algorithm was used, and the result was visually inspected by the interventionalist.

Endovascular device deployment

The participant was admitted to the Royal Melbourne Hospital the evening prior to the procedure and CT head and neck with contrast was performed as a baseline non-invasive venography study. The participant was placed under general anaesthesia and the angiography procedure was commenced. The co-registration of fMRI of data points on a structural MRI were used to generate an anatomical target using the roadmap function utilising the contrast-enhanced rotational 3D-DSA. A working view on the lateral plane on one image intensifier was set and utilised to overlay the roadmap with the anatomical targets (A, P and M1). The internal jugular vein was visualised under ultrasound guidance and punctured immediately above the clavicle, in between the two heads of the sternocleidomastoid muscle. A 6-French sheath (Pinnacle, Terumo) was exchanged over a microwire into the jugular vein. 5000 units of intravenous heparin were administered. Under DSA visualisation a coaxial catheter system (Fathom 16 microwire, Boston Scientific, MN; 3Max, 6-French Benchmark, Penumbra, CA) was advanced to the target location in the superior sagittal sinus. Venous tortuosity due to arachnoid granulations had been anticipated following their visualisation on the baseline CT venography. This resulted in minor resistance to the advancing 6-French catheter. Once the catheter was in position, the stent electrode array (Stentrode, Synchron, CA) was preloaded into a custom designed 4-French delivery sheath with radio-opaque tip (Synchron, CA), flushed with normal saline and advanced inside the guiding catheter. The delivery sheath was advanced to a position 10 mm beyond anatomical target A. The 6-French guide catheter was

retracted to the proximal superior sagittal sinus, leaving the delivery sheath in position. The delivery sheath was then retracted and positioned to match anatomical target A with the distal marker. The stent electrode array was then unsheathed, utilising the high radio-opacity of the cable to ensure correct positioning during deployment in the superior sagittal sinus with symmetric wall apposition (**Fig. 2; Video S1**). Repeat angiography demonstrated unimpaired blood flow through the Stentrode, with visualisation of an arachnoid granulation penetrating through a cell in the stent-head, resulting in anchoring of the device in position. The coaxial catheter system was removed, and gentle manual compression was held over the jugular vein to achieve haemostasis around the transvascular lead. The extension lead was unscrewed from the proximal portion, and the transmission lead exiting the vessel was tunnelled subcutaneously into a chest pocket. The proximal end was connected to the ITU (Synchron, CA) and the unit was implanted into the subcutaneous chest pocket immediately inferior to the left clavicle. Under sterile conditions in the angiography suite, the ETU was transiently placed above the ITU and the system check confirmed data was flowing. The participant was extubated in the angiography suite, monitored in the Intensive Care Unit and discharged home two days later.

DECODER

Parameter optimisation

Participant 1

Motor mapping task runs with a variety of movements were performed over the 12 sessions between day 50 and day 86 post-surgery. The data was used to determine the ideal strategy for BCI control and optimise the parameters of the preprocessing and classification layer based on decoding accuracy. Offline binary classification accuracy of left foot, right foot and right quadriceps movement attempt was assessed through random permutation. Across 50 iterations, a binary SVM was trained using a unique combination of training and validation dataset and its accuracy was tested on a fixed test set for each movement type separately (the test sets were initially randomly sampled and remained fixed through the iterations, and there were at least 810 samples to classify). The results revealed that the right quadriceps movement attempts yielded the highest accuracy averaged across the permutations (78.7±1.2%; mean±SD), compared to right (66.5±5.7%, Wilcoxon rank-sum test p=6.9006e-18) and left foot tapping attempts (55.5±2.3%, p=6.6045e-18; **Fig. S5**). Thus, we focused on the right quadricep movement attempts for future sessions. Between sessions 12 and 13, several typing tasks were performed using this decoder to optimise the parameters of the click-logic layer in the decoder. The decoder parameters were fixed from session 13 (day 92 post-surgery). All hyperparameters, except for C and γ of the SVC were manually optimised.

Oxley TJ, *et al. J NeuroIntervent Surg* 2020;0:1–7. doi: 10.1136/neurintsurg-2020-016862

Participant 2

Based on acquired knowledge from participant 1, it was deemed that direct visual feedback of features may help with training. However, high dimensional features that worked well for the SVM could not be visualised. Considering these factors, along with the success of extending binary classification events into two discrete outputs based on duration of control (i.e., click-logic layer), we employed a threshold decoder that took a 1D average spectral feature as an input that could be directly visualised. The ideal control strategy, feature channels and frequency bands described above were chosen based on the highest correlation values between the motor mapping tasks and spectral power of specific bipolar pair channels calculated from specific movement attempt types in session 1. The participant practiced controlling the 1D average spectral feature across the threshold levels with direct visual feedback, and the normalization constants and threshold values were fine-tuned session to session. The participant could also manually calibrate the normalization constants himself by clicking on the F11 key when using the system, which took 30 s.

General design

Raw data was sampled at 2 kHz per channel and was passed through the decoder comprised of three layers, preprocessing layer, classification layer, and click-logic layer (**Fig. S2**). The preprocessing layer removed large artifacts and disconnection events using thresholds in temporal and spectral domain and extracts spectral power as features. The classification layer predicted whether the features represented the state of rest or movement-attempts. The click-logic layer translated sequences of prediction events from the classifier into three outputs, no click, short click and long click. Hyperparameters of the decoders were manually tuned through trial and error and exploring the motor mapping task data. Participant specific settings for the decoder used for testing are provided below.

Preprocessing layer

For participant 1, the spectral features were extracted from a 100 ms window at 100 ms strides (i.e., every 100 ms). To capture neural correlates of right quadriceps movement attempts, the data from channels 4, 10 and 13 were re-referenced to channel 16 then passed through a 50 Hz notch-filter for line-noise removal and a 4-30 Hz second second-order Butterworth bandpass filter. Then, the decibel normalized spectral power of 1 Hz bins between 4-30 Hz were calculated using the Thompson multi-taper method[7]. Finally, the data bins were passed through a 1 s boxcar filter (across time), resulting in 78 features (3 channels x 26 frequency bins) per current data bin.

For participant 2, the spectral features were calculated from a 1000 ms window at 100 ms strides. To capture neural correlates of left foot movement attempts, the data from channels 6, 8, 10, 11 and 13 were re-referenced to channel 9, then, passed

through a 50 Hz notch-filter and a 4-200 Hz second-order Butterworth bandpass filter. Then, the decibel normalized spectral power of 5 Hz bins between 12-70 Hz were calculated using the Thompson multi-taper method. These features were averaged, then passed through a 500 ms boxcar filter resulting in 1 feature per current data bin.

Classification layer

For participant 1, ten manually selected right quadriceps motor mapping task runs between day 68 and 85 post surgery were used to train a binary support vector machine (SVM). Separate datasets were used to train (24 trials), tune hyperparameters (18 trials) and test (16 trials) the SVM. The SVM was trained with gaussian radial basis functions. The optimal hyperparameters C and gamma (γ) were chosen such that they maximise the F1-score on the validation set. The test set was withheld from training and tuning the SVM and used only to evaluate the accuracy of the trained SVM. The SVM layer z-normalized the data per channel, per frequency bin, using the constants calculated from the training data, then, predicted the state of given data bin as either rest or movement-attempt.

For participant 2, a threshold classifier was used, where the classifier predicted a movement-attempt state if the feature signal reached a given threshold value. Low and high threshold levels were manually tuned, where the former was closer to the baseline than the latter. If the system detected that the participant was typing by monitoring keystrokes, the threshold level was automatically set to the lower level. The threshold level defaulted back to high if typing was not detected for 15 s and at all other times. This design was intended to ease the criteria for typing where more consecutive click events were expected compared to general computer control.

Click-logic layer

For both participants, the predictions from the classification layer were passed through the click-logic layer which translated the sequences of classification predictions into three command outputs; no click, short click, and long click. Short clicks were generated when 3-9 consecutive movement-attempt predictions were immediately followed by a rest prediction. Long clicks were initiated on the 10th consecutive movement attempt predictions and the command was released on the subsequent rest prediction. This design allowed the participants to "click-hold-and-release" and control the screen magnification function for making fine-scale selections. All other events resulted in no clicks.

Multiclass classification

Offline analysis revealed above chance-level multiclass classification. For participant 1, signals recorded on channels 4, 10 and 13 from the right hand and right quadriceps motor mapping data were re-referenced to channel 16. Normalised spectral power of 2 Hz bins between 4-30 Hz, 60-80 Hz and 120-180 Hz were

extracted as features to classify rest, right quadriceps and right hand movement attempts. Rest period was defined as -4 s and -1 s from the attempt cue onset, and movement attempt period was between 1 s-4 s. Data window size was 500 ms with a 100 ms stride, resulting in 30 rest samples and 30 movement attempt samples per trial, per movement type. SVM training/tuning and testing set were randomly permutated 50 times without sequence repeats for cross validation of decoder performance. There were 19200 training and 4800 testing samples from mutually exclusive set of recordings per iteration. Across 50 iterations, the median precision, recall and F1-score were 0.30 (0.29-0.31), 0.66 (0.64-0.68) and 0.41 (0.40-0.43) for rest; 0.78 (0.77-0.80), 0.54 (0.53-0.54) and 0.64 (0.62-0.65) for right quadriceps; 0.87 (0.84-0.88), 0.53 (0.52-0.54) and 0.65 (0.64-0.66) for right hand; and 0.65 (0.64-0.66), 0.58 (0.56-0.59) and 0.57 (0.56-0.58) overall. All median values, except for rest precision, were higher than the 3-class chance-level of 0.35 derived using a binomial cumulative distribution with sample size of 4800 ($\alpha = 0.001$; **Fig. S5A**)[3]. The process was repeated for participant 2, except signals recorded on channels 4, 6, 8, 10, 13 and 14 from the left foot and right hand motor mapping data were re-referenced to channel 9 to classify between rest, left foot and right hand movement attempts. There were 8640 training and 2160 testing samples per iteration. Across 50 iterations, the median precision, recall and F1-score were 0.80 (0.78-0.81), 0.73 (0.71-0.75) and 0.76 (0.75-0.77) for rest; 0.61 (0.59-0.64), 0.66 (0.64-0.68) and 0.64 (0.62-0.65) for left foot; 0.42 (0.38-0.46), 0.48 (0.45-0.50) and 0.45 (0.42-0.48) for right hand; and 0.61 (0.59-0.63), 0.62 (0.61-0.64) and 0.62 (0.59-0.63) overall. All median values were higher than the 3-class chance-level of 0.36 derived using a binomial cumulative distribution with sample size of 1920 ($\alpha = 0.001$; **Fig. S5B**).

TASKS AND DIGITAL DEVICE CONTROL

The participants achieved task and real-world device control by controlling the cursor using an eye-tracker and no, short, and long click actions using the motor prosthesis through alternate access programs (Communicator-5, and Windows Control, Tobii Dynavox). For participant 2, the direct visual feedback was turned off when practicing system control. For the typing task, keys on a virtual keyboard could be pressed by moving the cursor to the target and clicking on the keys using either the short or long click actions. For the email, texting, shopping and finance task and for home-use, a mouse action type could be chosen from a selection bar and the action could be performed by moving the cursor to the target using the eye-tracker and controlling them with the short click or the long click. The long click allowed the participant to zoom into the screen and perform the chosen mouse action on the target item, in turn, allowing the participant to interact with small items on the screen without having to change the screen resolution or use limited field-of-view applications.

Performance testing

The accuracy of the selections made, $click\ selection\ accuracy$, was defined as:

$$click\ selection\ accuracy = \frac{S_{total} - S_{error}}{S_{total}}$$

where S_{total} is total number of selections and S_{error} is the total number of errors. Typographical, spelling, and eye-tracker related errors that may have been intentionally selected were counted as errors.

The rate of erroneous selections made, $click\ selection\ errors$, was defined as:

$$click\ selection\ errors = 1 - click\ selection\ accuracy$$

$Click\ selection\ accuracy$ and $click\ selection\ errors$ are presented as percentages in results.

The rate of correct characters per minute or $CCPM$, was defined as:

$$CCPM = \frac{S_{total} - S_{error}}{t}$$

where t is the sum of the elapsed time to make all the selections in minutes.

Bits/trial, B, was defined as per[4]:

$$B = log_2\, N + P\ log_2\, P + (1 - P)\ log_2\ \left(\frac{1 - P}{N - 1}\right)$$

where N is the total number of symbols to select from, P is the probability that the symbols are correctly chosen and is equal to $click\ selection\ accuracy$ per trial. Equal error probability is assumed for each symbol (i.e., $\frac{1-P}{N-1}$).

The information transfer rate, ITR, was calculated as:

$$ITR = \frac{B}{t_{trial}}$$

where t_{trial} is the average time taken to make a single selection in seconds.

B and ITR were calculated for the motor neuroprosthesis + eye-tracker, by setting N as the total number of keys on the virtual keyboard used ($N = 31$). The isolated contribution of the motor neuroprosthesis to B and ITR was estimated by setting Nas the total number of commands actionable using the decoder ($N = 3$) as the number of available commands persists across keys.

Instrumental Activities of Daily Living (IADL) tasks

The texting task involved opening the WhatsApp from the desktop, clicking on the 'contact search' button, typing the recipient's name, clicking on the recipient's contact profile, typing "hello" and clicking the 'send' button. The email task involved opening Google Chrome from the desktop, clicking on the shortcut icon to Gmail, the 'compose' button, and the address bar, typing in the recipient's email, clicking on the subject bar, typing "letter" and the email body, typing "G'day from <location>!" (<location> was replaced with the participant's home town), clicking on the emoji button, the smiley-face emoji icon, and the attachment button, searching and attaching for a pre-defined file in the attachment prompt window, clicking the "Send" button on the email webpage, and then closing the browser. The shopping task involved opening Google Chrome, navigating to

amazon.com.au, searching for "jumper", clicking on a desired item, picking a size, adding the item to the cart, searching for "ramp", clicking on a desired item, adding the item to the cart, then clicking on 'check out'. No items were purchased. The finance task involved opening Google Chrome, navigating to their internet banking website, logging on and checking the balance. Given the qualitative nature of these tasks, the performance was measured as either successful or unsuccessful.

SUPPLEMENTARY TABLES AND FIGURES

Table 1. Inclusion and exclusion criteria

Inclusion criteria	**Exclusion criteria**
Clinical diagnosis of spinal cord injury (SCI), amyotrophic lateral sclerosis (ALS), stroke or muscular dystrophy.	Has dementia or cognitive impairment sufficient to impair capacity to provide informed consent or which could impact ability to comply with investigational requirements (eg: MMSE <24, ECAS or other determination made by Investigator)
Diagnosed for at least six (6) months and if SCI, at least twelve (12) months	For ALS participants, has NOT had a formal capacity assessment by a professional with experience in capacity assessment (psychiatrist, neurologist, psychologist) within 90 days of Screen1 visit, which assesses capacity to consent and excludes Frontotemporal dementia
Life expectancy of at least twelve (12) months in the opinion of the treating physician	Chronic oral or intravenous steroids or immunosuppressive therapy or other therapy/clinical condition that severely reduces immunity
Pattern of complete or incomplete quadriplegic weakness with associated functional impairment, with specific cord level MRC weakness of at least: • C5 <= 4/5 grade • C6 <= 2/5 grade • C7-T1 <= 1/5 grade *If the participant has a diagnosis of ALS the participant may have 4/5 grade weakness with functional impairment and must report subjective decline over preceding four months*	Based on the enrolling physician's opinion, has unrealistic expectations regarding the possible benefits, risks and limitations associated with the implantation or surgical procedures
Participants with ALS must have: • Confirmed clinical diagnosis of "Clinically Definite ALS", "Clinically Probable ALS", "Clinically Probable-Laboratory Supported ALS" not caused by HIV. • Advanced Care Directive in place before insertion of device. • Assessment by specialist supporting service regarding respiratory function and potential use of non-invasive ventilation	Has been hospitalized for a psychiatric condition with the preceding two (2) years or has had a history of psychosis within the preceding two (2) years
No conditions, including an eye movement disorder, that would prevent the use of eye tracking software and has a level of vision that will not impede viewing of screens and visualisations	Is deemed unsuitable by a specialist anaesthesiologist or respiratory physician to undergo a general anaesthetic (ie FVC < 60%)
Has normal venous sinus anatomy, with two patent jugular veins (of sufficient size for the device) and bilateral patent transverse sinuses as evidenced by MR venography (MRV) or CT venography (CTV) within the last six (6) months or if vascular anatomy is unknown, is willing to undergo an MRV or CTV assessment to assess vascular suitability for endovascular device placement	Has findings on MRV deemed incompatible, by an experienced neurointerventionalist, with device implantation in the SSS [eg: isolated dominant, superior anastomotic vein (vein of Trolard)]
Evidence of activation, under fMRI testing, of motor cortical areas adjacent to the superior sagittal sinus	Has a contraindication to angiographic imaging, including chronic kidney injury (CKI -eGFR < 60mls/min)

	Has a history of Deep Vein Thrombosis (DVT) or on hormone therapy (eg: HRT)
	Has any bleeding disorders (tests required if clinical status unknown) or is resistant to aspirin and/or clopidogrel or has any contraindication that precludes antithrombotic treatment
	Has an active implanted stimulation device (eg: pacemaker, deep brain stimulator, spinal cord stimulator)

Table 2. Trial average system control performance

	Trials (Words)	Selections	Errors	Duration (s)	Duration/ Selection (s)	Click selection accuracy (%)	Click selection error (%)	CCPM	MN Bit/trial	MN ITR bits s^{-1}	MN + ET Bit/trial	MN + ET ITR bits s^{-1}	Text task	Email Task	Shopping Task	Finance Task
Par. 1													Success	Success	Success	Success
Sum	129	748	68	3211.23	-	-	-	-	-	-	-	-	12	5	2	2
Mean	-	-	-	24.89	4.34	92.63	7.37	13.81	1.31	0.32	4.39	1.08	-	-	-	-
SD	-	-	-	9.71	1.33	15.22	15.22	4.33	0.43	0.13	0.96	0.36	-	-	-	-
Min	-	-	-	9.91	2.17	0.00	0.00	0.00	0.17	0.04	0.05	0.01	-	-	-	-
Q1	-	-	-	17.96	3.35	87.50	0.00	10.96	0.92	0.24	3.80	0.86	-	-	-	-
Median	-	-	-	23.44	3.90	100.00	0.00	13.44	1.58	0.30	4.95	1.05	-	-	-	-
Q3	-	-	-	29.90	5.21	100.00	12.50	16.09	1.58	0.41	4.95	1.30	-	-	-	-
Max	-	-	-	73.78	9.22	100.00	100.00	24.22	1.58	0.64	4.95	2.00	-	-	-	-
Par. 2													Success	Success	Success	Success
Sum	95	569	64	2040.32	-	-	-	-	-	-	-	-	5	1	1	1
Mean	-	-	-	21.48	3.66	93.18	6.82	20.10	1.33	0.46	4.43	1.57	-	-	-	-
SD	-	-	-	16.15	2.36	14.47	14.47	10.28	0.46	0.27	1.01	0.82	-	-	-	-
Min	-			4.04	1.14	22.22	0.00	2.86	0.00	0.00	0.37	0.11	-	-	-	-
Q1	-	-	-	11.54	2.17	88.19	0.00	12.27	0.94	0.28	3.85	0.98	-	-	-	-
Median	-	-	-	17.35	3.10	100.00	0.00	17.73	1.58	0.41	4.95	1.40	-	-	-	-
Q3	-	-	-	25.12	4.54	100.00	11.81	26.50	1.58	0.63	4.95	2.11	-	-	-	-
Max	-			93.93	18.79	100.00	77.78	48.94	1.58	1.29	4.95	4.04	-	-	-	-

SD = standard deviation; CCPM = correct characters per minute; ITR information transfer rate; MN = motor neuroprosthesis; ET = Eye tracker

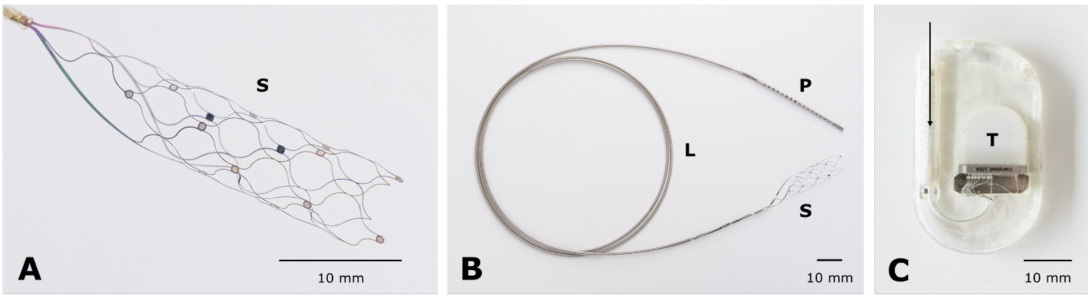

Figure S1. Implantable components

Panel A shows the stent-head (S). Panel B shows the Stentrode stent-head (S), transmission lead (L), and proximal connector (P). Panel C shows the internal telemetry unit (ITU) showing the location of the Stentrode insertion (arrow) and the hermetically encapsulated telemetry chip (T).

Oxley TJ, *et al. J NeuroIntervent Surg* 2020;0:1–7. doi: 10.1136/neurintsurg-2020-016862

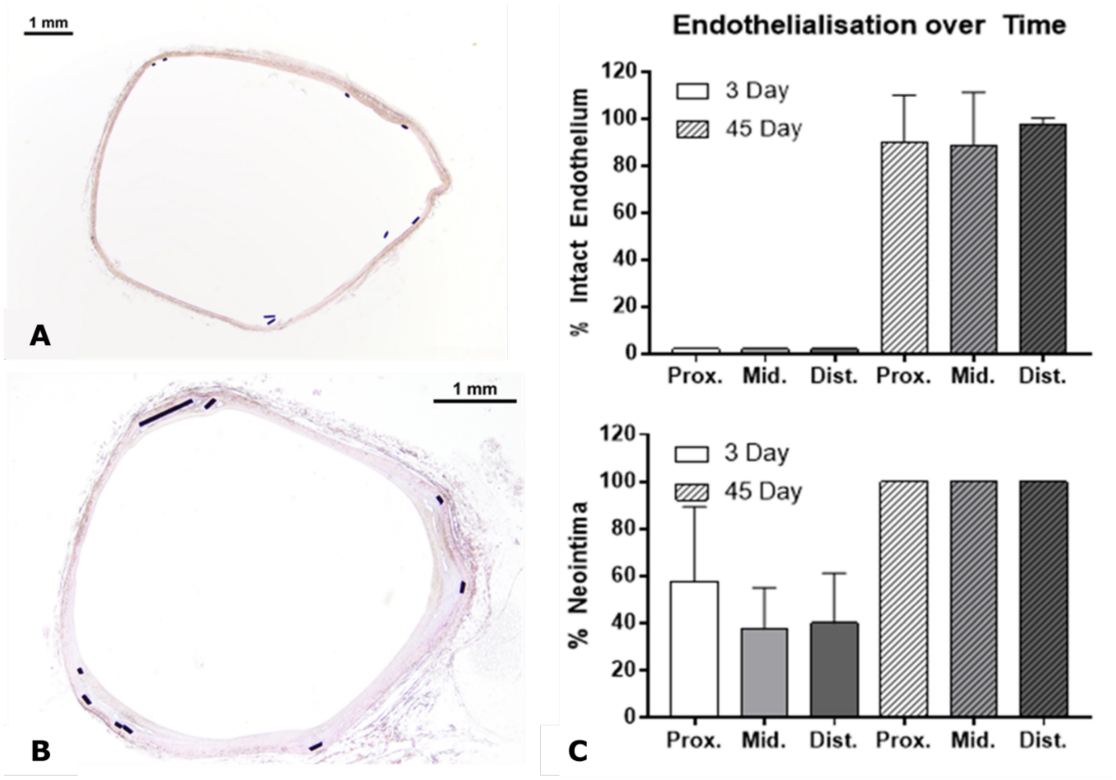

Figure S2. Endothelialisation of Stentrode implanted in chronic animal trial
Histopathological hematoxylin and eosin stained sections of a sheep vessel implanted with a Stentrode implanted for durations of A) 3 days and B) 45 days showing vessel patency and incorporation of stent struts by 45 days. C) Histopathologically assessed endothelium as a function of implant time for stent segments assed at the proximal (Prox., white), middle (Mid., grey) and distal (Dist., dark grey) stent locations for animals implanted for 3 days (n=2, clear bars) and 45 days (n=4, dashed bars). C) The percentage of intact endothelium was 0% across all positions for both animals assessed 3 days post implant, increasing to 90.0±10.0%, 88.8±11.3%, and 97.5±1.4% (mean±SEM) for the proximal, middle and distal sections, respectively for animals implanted for 45 days. D) The percentage of intima lined by an acute fibrin layer was 57.5±22.5%, 37.5±12.5%, and 40.0±15.0 (mean±SEM, n=2) for the proximal, middle and distal sections, respectively, in animals implanted for 3 days. Stent struts were covered (100%) in neointima in all animals implanted for 45 days across all positions.

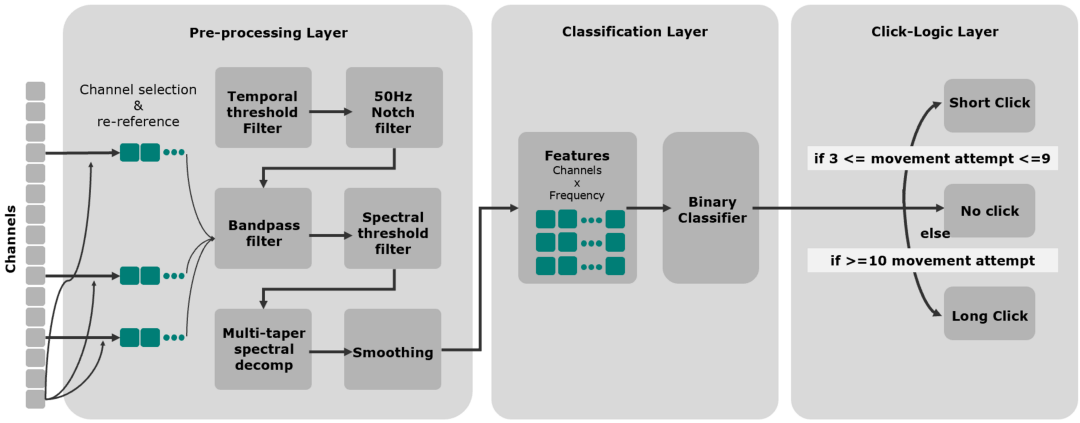

Figure S3. Custom decoder

The decoder takes a window of data every 100 ms from selected feature channels, then passes it through the preprocessing, classification, and click-logic layer. The preprocessing layer extracts normalised spectral power as features. The classification layer then predicts the current set of features as either rest or movement-attempt. Finally, the click-logic layer outputs no clicks, short clicks, or long clicks, based on the sequence of classification outputs. If between 3 and 9 consecutive movement-attempts are immediately followed by a rest classification, short clicks are generated. Long clicks are initiated upon the 10th consecutive movement attempt classifications and are released upon a subsequent rest classification. All other sequences of events result in no clicks.

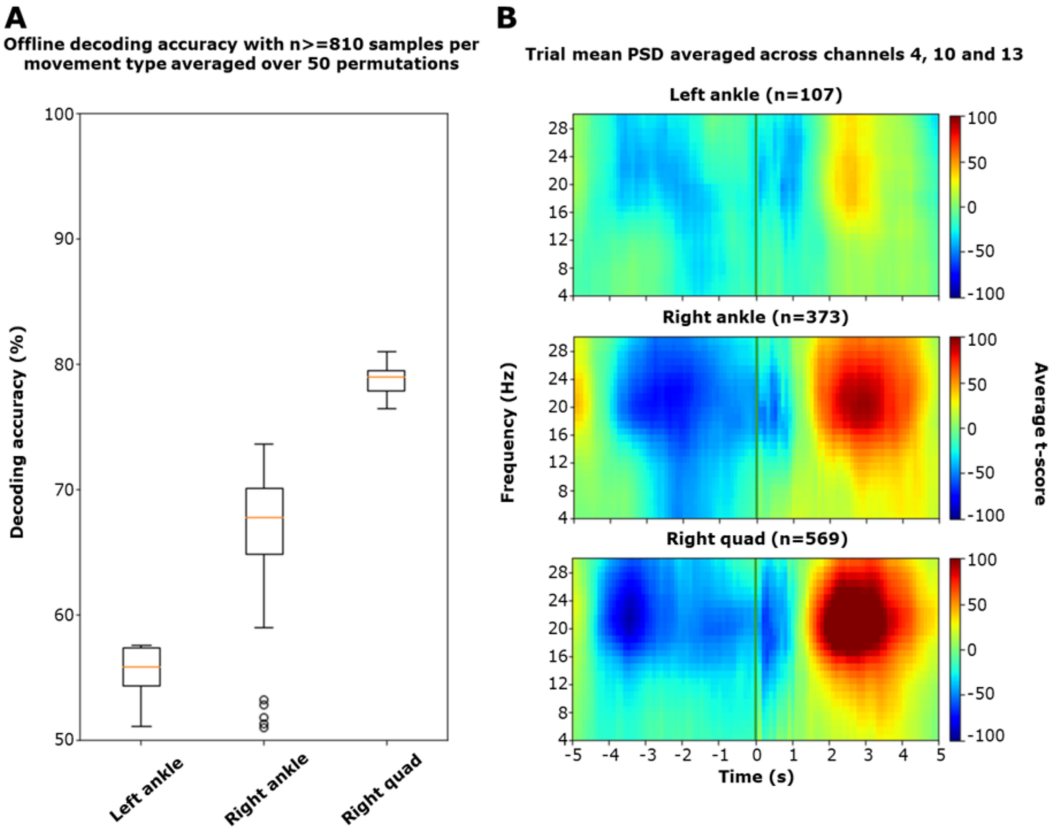

Figure S4. Motor mapping of movement-attempts

Panel A shows a box plot of offline decoding accuracy of various movement-attempts performed by participant 1 during motor mapping task in sessions 1-12, averaged across 50 random permutations. Unique combinations of runs were chosen for SVM training and tuning at each random permutation. The test set runs were fixed after initial randomisation with at least 810 samples. Orange lines depict medians and the box outlines the 1st and 3rd quartile, whiskers depict range, and circles depict outliers. Panel B shows the trial mean spectrogram during motor mapping task as t-scores for ease of cross-frequency visualisation, averaged across feature channels 4, 10 and 13. Green line depicts the transition point from attempt to rest blocks.

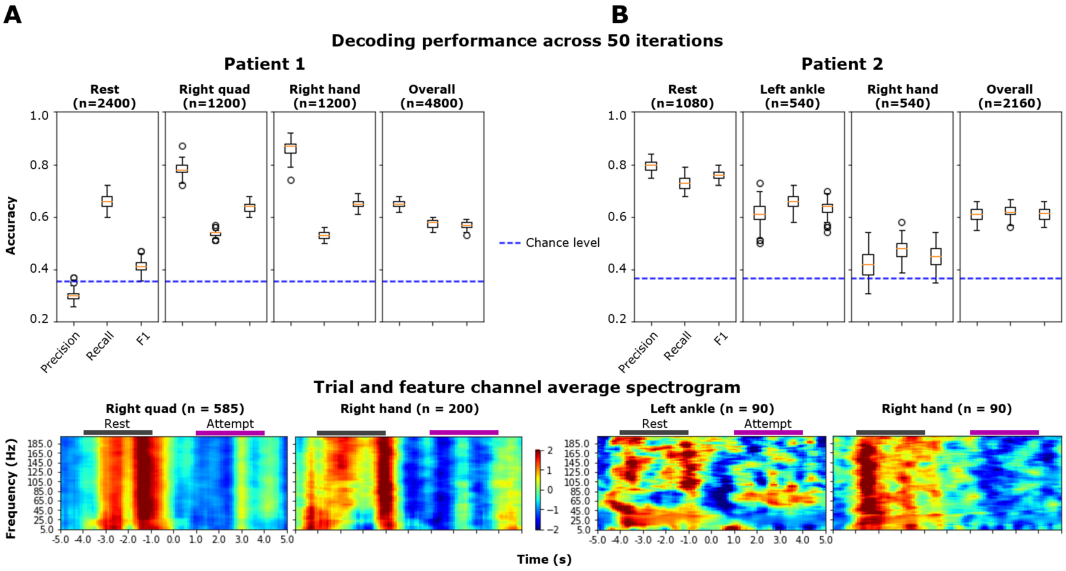

Figure S5. Classification of various movement-attempt types

Panel A shows the box plots of offline multiclass decoding performance metrics across 50 random permutations for patient 1 and Panel B for patient 2. Unique combinations of runs were chosen for SVM training/tuning and testing at each random permutation. The orange line depicts the median and the box outlines the 1st and 3rd quartiles, and whiskers depict the range. The blue dashed line shows the 3-class chance-level derived using a binomial cumulative distribution at alpha=0.001. n above box plots denotes number of samples. The spectrograms show the z-normalised spectral power evolution centred around the movement-attempt cue onset. n above spectrograms denotes the number of epochs.

SUPPLEMENTARY VIDEOS

Video S1. Neurointerventional procedure and device implant vignette

https://synchron.egnyte.com/dl/5WM6lOmgug

Video S2. Motor neuroprosthesis performance and utilisation vignettes

https://synchron.egnyte.com/dl/NhihAUzACw

Vignette 1 - Remote texting caregiver	0 mins
Vignette 2 - Playing music	1 mins 40 secs
Vignette 3 - Internet browsing	2 mins 28 secs
Vignette 4 - Typing task: participant 1	3 mins 10 secs
Vignette 5 - Typing task: participant 2	5 mins 05 secs
Vignette 5 - Text task	6 mins 10 secs
Vignette 6 - Email task	7 mins 20 secs

REFERENCES

1 Yoo PE, Oxley TJ, John SE, *et al*. Feasibility of identifying the ideal locations for motor intention decoding using unimodal and multimodal classification at 7T-fMRI. *Scientific Reports* 2018;**8**:15556. doi:10.1038/s41598-018-33839-4

2 Yoo PE, Hagan MA, John SE, *et al*. Spatially dynamic recurrent information flow across long-range dorsal motor network encodes selective motor goals. *Human Brain Mapping* 2018;**39**:2635–50.

3 Combrisson E, Jerbi K. Exceeding chance level by chance: The caveat of theoretical chance levels in brain signal classification and statistical assessment of decoding accuracy. *J Neurosci Methods* 2015;**250**:126–36. doi:10.1016/j.jneumeth.2015.01.010

4 Wolpaw JR, Ramoser H, McFarland DJ, *et al*. EEG-based communication: improved accuracy by response verification. *IEEE Trans Rehabil Eng* 1998;**6**:326–33. doi:10.1109/86.712231